CHEMISTRY
A European Journal

A Journal of
ChemPubSoc Europe

Accepted Article

Title: Differential Gelation and Self-Sorting Properties of Two Isomeric Polyamides Due to the Parallel vs Anti-Parallel Alignment of Backbone Dipoles

Authors: Chui-Fan Leung and Hak-Fun Chow

To be cited as: *Chem. Eur. J.* 10.1002/chem.201605819

Link to VoR: http://dx.doi.org/10.1002/chem.201605819

Supported by
ACES

WILEY-VCH

10.1002/chem.201605819

WILEY-VCH

Differential Gelation and Self-Sorting Properties of Two Isomeric Polyamides Due to the Parallel *vs* Anti-Parallel Alignment of Backbone Dipoles

Chui-Fan Leung,[a] and Hak-Fun Chow*,[a]

Dedicated to Prof. Dieter Seebach on the occasion of his 80th birthday

Abstract: Two isomeric bottlebrush polyamides **P-1** and **A-1** having the same repeating monomer dipole units aligned along the polymer backbone in pseudo-parallel and pseudo-anti-parallel, respectively, were synthesized and characterized. Both polymers can form thermoreversible gels with aromatic solvents but **P-1** was found to show inferior gelation strength as compared to that of **A-1**. Furthermore, despite their close structural resemblance, a 1:1 mixture of the **P-1** and **A-1** polymers was shown to exhibit self-sorting in the gel state. Gel formation was found to be a kinetically trapped process via H-bonding, π−π stacking interactions and side chain interdigitation. The differential gelation and self-sorting properties can be explained by the local dipole-dipole interactions originated from the different modes of backbone dipole alignment. In single gel systems, the antiparallel-aligned dipoles in **A-1** facilitated a more compact molecular packing due to the enthalpically more favorable polymer chain association. On the other hand, the parallel-aligned dipoles in **P-1** gave rise to a less stable head-to-head packing, which had difficulties to convert to the more stable head-to-tail packing in a kinetically trapped environment. In the mixed gel system, it is the unfavorable hetero-polymer mismatch dipole-dipole interaction that inhibited the mixing of the **A-1** and **P-1** polymers and led to self-sorting.

Introduction

Self-assembly of macromolecules is a universal, complex yet crucial phenomenon. It is a spontaneous behavior that produces order in a system. Polymer crystallization, gelation, adsorption, and phase separation can all be viewed as different manifestations of macromolecular self-assembly. Mechanistically, this process is based on the collective and cooperative non-covalent interactions of polymer molecules. Understanding the self-assembly of bio-macromolecules, such as that of amyloidogenic proteins/peptides, occurred in living systems can give us a better clue on the cause of many neuro-degenerative diseases.[1] In materials science, studying the aggregation of conjugated polymers can help improve their optoelectronic properties, and can illuminate ways to fabricate new materials with unique functions.[2]

The gelation of macromolecules can be considered as a special case of self-assembly, in which the molecules themselves not just interact with each other to form aggregates, but the resulting assemblies can create a network that spans the volume of the liquid medium, and immobilizes the solvent molecules to form solid-like gels. Depending on the nature of the driving force that leads to gel formation, polymer gels can be classified as chemical and physical gels. In the former case, network formation is established through strong covalent linkages of polymer chains, and therefore the resulting gel cannot be reversibly converted back to the sol.[3] In contrast, the driving forces that hold physical gels are non-covalent in nature, which are weaker and can be broken down easily. Hence, the gel can return to the sol state at elevated temperature. In the literature, most polymer gels are chemical ones which are prepared by extensive crosslinking of polyfunctional monomers. On the other hand, examples of polymer physical gels are fewer.[4] In contrast to low molecular weight gelators, in which the gelation mechanism has been extensively studied,[5] the gelation mechanism of polymer physical gels is less understood. This is an intrinsic problem when dealing with the structurally more complex polymer systems, as there are many parameters, such as multiple functional group and side-chain interactions, backbone conformation and chain mobility that are in action. We are interested in deciphering the gelation mechanism of dendronized oligo- and poly(amide-triazole)s, and have identified several factors that can influence their gelation properties.[6] Hence, it was shown that the gel-to-sol melting temperature (T_m) of a series of H-bond-mediated oligo(amide-triazole) gels increased monotonically with increasing number of amide units along the polymer chain (Figure 1a).[7] Poly(amide-triazole)s with a structurally more rigid backbone held by intramolecular H-bonds were more likely to be a gelator than structural similar poly(amide-triazole)s without backbone rigidity (Figure 1b).[8] In a study of the polymer side chain effect, it was noted that the size of the side chain of a series of poly(amide-triazole)s had an impeding effect on the strength of self-association (Figure 1c).[9] Hence, a bulky side chain led to polymer dissolution and a small side chain led to polymer precipitation, and that an intermediate size side chain was the optimal one to confer the resulting poly(amide-triazole) with gelating properties. More intriguingly, the relative orientation of the triazole dipole units along the polymer backbone also played a subtle role in controlling their supramolecular properties (Figure 1d).[10] Hence, the dendronized poly(amide-triazole) with the triazole dipoles aligned in pseudo-parallel (hereafter parallel) fashion along the polymer backbone showed different organogelating properties as compared to the corresponding isomeric dendronized poly(amide-triazole) with the triazole dipoles aligned in pseudo-antiparallel (hereafter antiparallel) manner. It was proposed that the presence of a macro-dipole

[a] Ms C.-F. Leung, Prof. Dr. H.-F. Chow
Department of Chemistry and Center of Novel Functional Molecules
The Chinese University of Hong Kong
Shatin, NT, Hong Kong SAR
E-mail: hfchow@cuhk.edu.hk

Supporting information for this article is given via a link at the end of the document.

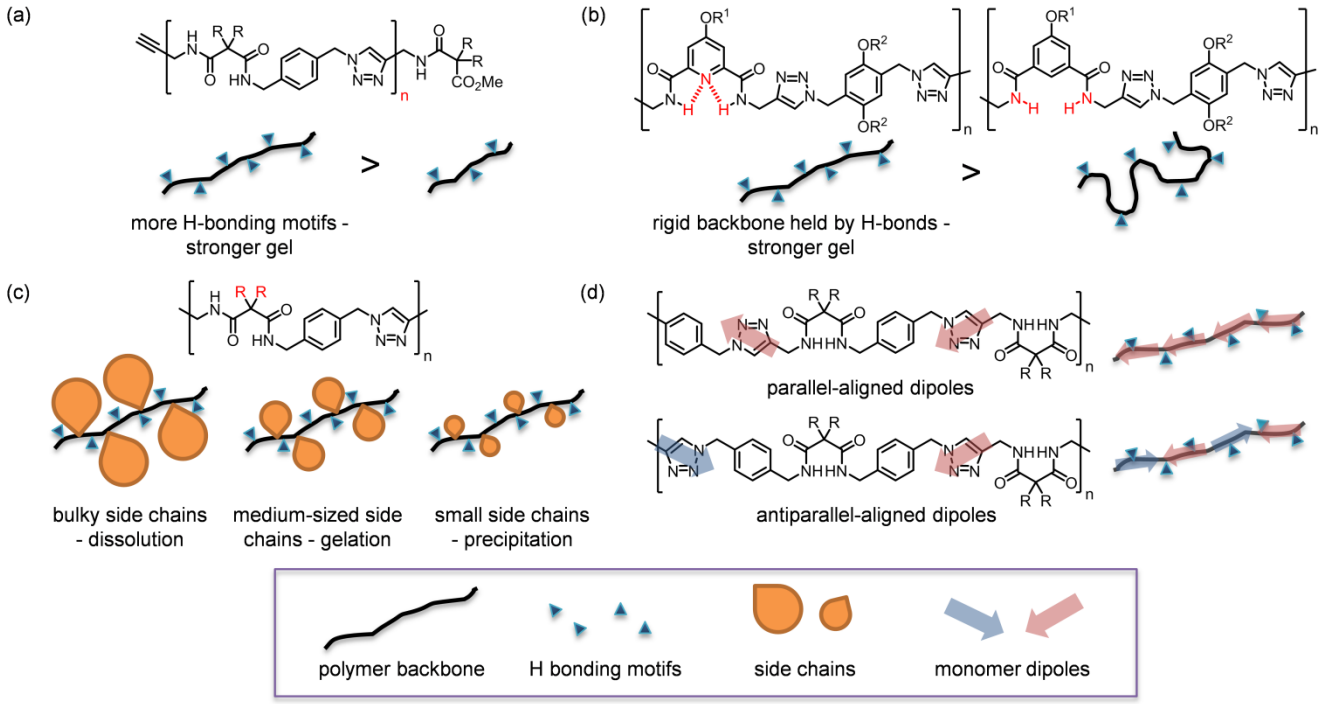

Figure 1. Examples of oligo- and poly-(amide-triazole)s that exhibit supramolecular gelation properties.

(resulting from the cumulative effect of the parallel-aligned dipoles) in the parallel-aligned polymer and the lack of such a macro-dipole in the antiparallel-aligned polymer led to the observed differential gelation behavior. The cumulated macro-dipole concept had been used to rationalize the quaternary structure[11] and enhanced catalytic property[12] of many α-helical proteins. However, recent research findings questioned the validity of the macro-dipole concept, and pointed out that the local dipole-dipole interaction is much more important to account for the observed protein properties.[13] In this context, it is deemed necessary to revisit the mechanism of dipolar polymer gelation by focusing on the local dipole-dipole interactions. In this paper we reported new and interesting findings on this polymer backbone dipole alignment effect by studying the gelating and self-sorting properties of two isomeric polyamides, namely **P-1** and **A-1**, with *para*-alkoxybenzamide dipole units aligned in parallel and antiparallel fashions, respectively, along the polymer backbone (Figure 2a). It was found that (a) both polymers are good organogelators of aromatic solvents, but they exhibit differential gelation strength, (b) gel formation involves the kinetic trapping of polymer molecules, (c) the mode of polymer backbone dipole alignment has a strong effect on the gelation strength; the difference in their gelation properties can be readily rationalized by the differential local dipole-dipole interactions arising from the parallel *vs* antiparallel dipole alignments, and agrees well with the corresponding enthalpic and entropic parameters obtained from differential scanning calorimetry (DSC) and diffusion wave spectroscopy (DWS), (d) despite their close structural similarity, the **P-1** and **A-1** polyamides exhibited self-sorting during mixed gel formation, and (e) the dipole-dipole interaction effect appears to be general; previously it was demonstrated that the effect was associated with the triazole unit, now it is also found with the *para*-alkoxybenzamide dipole. The results reported here highlight the multifaceted nature of polymer physical gels, in which not only thermodynamic factors, but kinetic ones are also of importance in determining their gelation mechanism. Furthermore, the subtle but influential backbone dipole alignment effect on the self-assembling and gelating properties of polymers, a factor that is of less significance in low molecular weight gelators due to the absence of molecular entanglement, is clearly demonstrated.

Results and Discussion

Design of polymer structure

In order to evaluate the cumulative effect of backbone dipoles on the supramolecular and gelation properties of the corresponding polymer, it is important to set out several key design principles. First, the backbone of the polymers should be relatively rigid in order to minimize back folding. A bottlebrush polymer architecture with several long alkyl side chains (*i.e.* R^1 and R^2) were installed to ensure the backbone will possess a relatively rigid conformation.[14] Second, the monomer dipole should be strong enough to enable its effect to be observed. Third, the

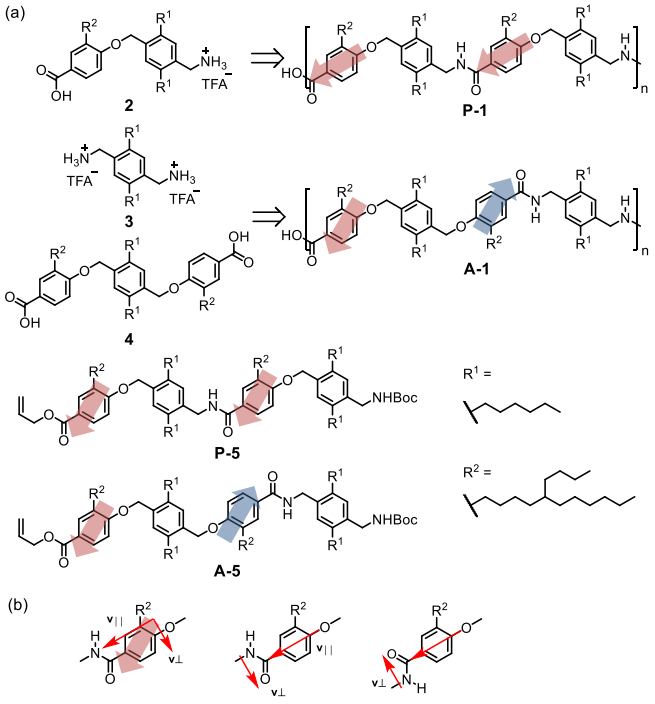

Figure 2. (a) Structure of parallel and antiparallel aligned polymers and dimers. (b) Orientation of the overall dipole and its $v_{\parallel}$ and $v_{\perp}$ components.

dipole parallel-aligned and anti-parallel-aligned polymers should be of similar molecular weight and distribution profile such that a meaning comparison can be made. After putting these into considerations, it was decided to use *para*-alkoxybenzamide as the dipole unit, which was calculated to have a dipole moment of 4.9 Debye according to DFT calculation [see Supporting Information (SI) section 1, Figure S1]. It is noted that the orientation of dipole moment of this unit does not coincide with that of the polymer backbone due to the vectorial contributions from both the amide CONH and the *para*-alkoxyaryl dipoles (Figure 2b). Nonetheless, the overall dipole could be resolved into two components; one of which ($v_{\parallel}$) is parallel (*i.e.* backbone dipole) and the other ($v_{\perp}$) is perpendicular to the polymer backbone.[15] It should be noted that orientation of $v_{\parallel}$ is fixed in space along with that of the polymer backbone, while that of $v_{\perp}$ can tumble as a result of rotational freedom of the aryl−C(O) bond. Hence, for both the **P-1** and **A-1** polymers, the density and the orientation distribution of the $v_{\perp}$ components are essentially the same. The differential gelation properties are therefore principally due to the difference of the orientation distribution of the $v_{\parallel}$ components (*i.e.* parallel *vs* antiparallel backbone dipole alignment). It is anticipated that the dipole moment will change slightly upon H-bonding, but the above conclusions remain the same. The resulting **P-1** polymer was prepared via condensation polymerization from an AB-type monomer **2**, while the corresponding **A-1** polymer was obtained from condensation copolymerization of AA-type **3** and BB-type monomers **4** (see SI section 2 for details). For comparison of the infrared absorption property, the corresponding parallel- and antiparallel-aligned dimers, **P-5** and **A-5**, respectively, were also synthesized.

Structural Characterization

1. Nuclear magnetic resonance spectroscopy. All compounds prepared were characterized by ^{1}H and ^{13}C NMR spectroscopy and, except **P-1** and **A-1**, by mass spectrometry. The spectroscopic data agreed well with the proposed structures. Due to their isomeric nature, the ^{1}H NMR spectra of **P-1** and **A-1** are very similar, though careful observation revealed the presence of some minor oligomeric species in **A-1** (see SI section 3, Figure S2). This was probably due to a slight deviation from the exact 1:1 reaction stoichiometry between the AA **3** and BB **4** monomers. Such lower molecular weight oligomers may facilitate in triggering the gelation of **A-1**, but should pose little influence on the thermodynamic and kinetic data obtained from the experiments since they are present in small amount.

2. Gel permeation chromatography (GPC). The two polymers were subjected to GPC analysis coupled to a multi-angle laser light scattering (MALLS) detector in order to obtain the molecular weight distribution and absolute molecular weight information (Figure 3 and Table 1). As disclosed in the introduction section, the gelation strength of the polymer is dependent on the total number of H bonding units in the polymer chain. However, since there is a plateauing effect once the number of H-bonding unit becomes very large (~20), therefore there is no absolute need to have the prepared polymers having exactly the same MW. As can be seen, the two polymers possessed similar GPC profiles, although that of **A-1** contained larger amount of low molecular weight oligomers. It should be noted that the relative % of the low molecular weight oligomers is exaggerated in the plot as the x-axis is on a logarithm scale of polymer M_w. The M_w (GPC based on PS standards) values of **P-1** and **A-1** were comparable (17.7 vs 14.6 kD), and their polydispersity indexes (PDI) were both around 2.0 – a typical value expected from a step-growth polymerization. The M_w values obtained from MALLS were found to be 18.0 and 16.2 kD for **P-1** and **A-1**, respectively.

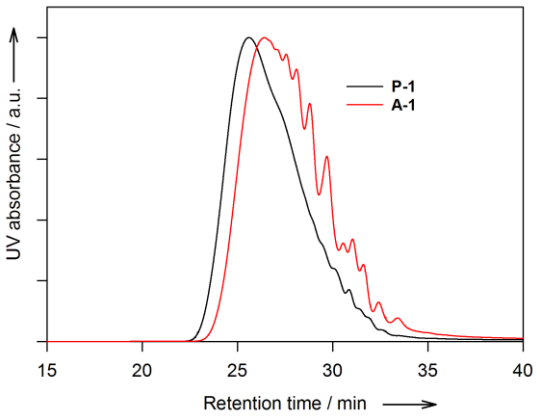

Figure 3. GPC profiles (THF, 40 °C) of **P-1** and **A-1** polymers.

Table 1. Molecular weights and PDI of **P-1** and **A-1** polymers.

	P-1		A-1	
	GPC-UV	GPC-MALLS	GPC-UV	GPC-MALLS
M_w (kD)	17.7	18.0	14.6	16.2
M_n (kD)	8.7	13.2	7.3	12.3
PDI	2.04	1.37	2.01	1.31

Organogelation property

1. Minimum gelation concentration and gel-to-sol transition temperature. The two target polymers were found to form strong organogels with most aromatic solvents (Table 2). The gels were prepared by ambient temperature cooling of boiling solutions of the polymer, and gelation generally took place within 5 min. The minimum gelation concentration (MGC) values of **A-1** are consistently lower than those of **P-1** in all aromatic solvents examined. A crude estimation of the gelation strength was obtained by plotting the gel-to-sol melting temperature (T_m) in *para*-xylene at different gelator concentrations, and the result also confirmed the better gelation strength of **A-1** (see SI section 5, Figure S4). It was noted that significant difference in the T_m (~30 °C) was found at a lower gelator concentration (3%). Hence, preliminary results indicated that the monomer dipole alignment did affect the self-association strength of the gel network.

Table 2. MGC values of **P-1** and **A-1** in various solvents.[a]

Solvent	P-1	A-1
THF	S	S
DMF	S	S
DMSO	S	S
CHCl3	S	S
Ethyl acetate	2% (OG)	5% (TG)
Chlorobenzene	5% (OG)	3% (CG)
ortho-Dichlorobenzene	S	S
Toluene	3% (TG)	1% (CG)
para-Xylene	3% (TG)	1% (CG)
Anisole	5% (TG)	2% (CG)

[a] S: very soluble; OG = opaque gel; TG = transluent gel; CG = transparent gel.

2. Fourier-transformed infrared spectroscopy (FT-IR). To confirm that H-bonding interaction was responsible for the gelation, the two polymer samples **P-1** and **A-1** as well as the non-gelating dimers **P-5** and **A-5** were subjected to FT-IR analysis (see SI section 6, Figure S5). The FT-IR spectra of the two dimers in 5% toluene solution showed two IR adsorptions at 3440 and 1668 cm^{-1}, which could be attributed to the non-H-bonded N−H and C=O amide stretching frequency, respectively. On the other hand, these two peaks were red-shifted to 3280 and 1628 cm^{-1} in the 3% polymer gels in toluene. Hence gelation was driven by H-bonding.

3. Differential scanning calorimetry (DSC). Having established that the backbone dipole alignment did have an effect on the self-assembly and hence the organogelating strength of the resulting polymers, the thermodynamic parameters of the gel-sol transitions were then extracted using DSC analysis. The DSC traces of toluene gel samples of **P-1** and **A-1** were shown in Figure 4. At 3.0 % gelator concentration, where both polymer samples were in the gel state, the heating profile of **P-1** showed one broad peak centered at 51.7 °C. The broadness of the peak reflected the heterogeneous micro-structure of the polymer gel. The DSC profile of **A-1** was more complex, giving two peaks at 53.5 and 64.7 °C. The peak at 64.7 °C was relatively sharp, suggesting this was due to the melting of a more crystalline state. These two prominent transition temperatures of **A-1** were both higher than that of **P-1**. For the 1.0% gel samples, the DSC curves were similar, even though **P-1** now appeared as a partial gel. It was noted that the melting peak at 65.7 °C of **A-1** was further sharpened. On the other hand, the DSC cooling curves (cooling rate = 1 °C/min) looked simpler. The gelation temperature (T_{gel}) now appeared at 35.9 and 32.3 °C for the 3% and 1% **P-1** samples, respectively. For the 3% and 1% **A-1** samples, the T_{gel} values were 56.5 and 54.3 °C, respectively. This result indicated the presence of hysteresis and is typical of physical gels,[16] highlighting that the formation of such polymer physical gels via ambient temperature cooling is a kinetic-trapping process.[17] Indeed, when the cooling rate was increased to ~4 °C/min in the DSC scans, the melting temperature of both **P-1** and **A-1** decreased by about 1−2 °C (see SI section 7.II, Figure S6). Apparently, the slightly faster cooling rate (4 °C/min) did not provide the polymer chains with enough time to search for a more stable crystalline state. The relatively complex DSC profiles also confirmed that the gel-sol process actually involved several phase transitions instead of a single one. This observation is consistent with the widely accepted model that polymer physical gels consist of crystalline regions (also known as junction zones) as well as amorphous regions composed of dangling chains.[18]

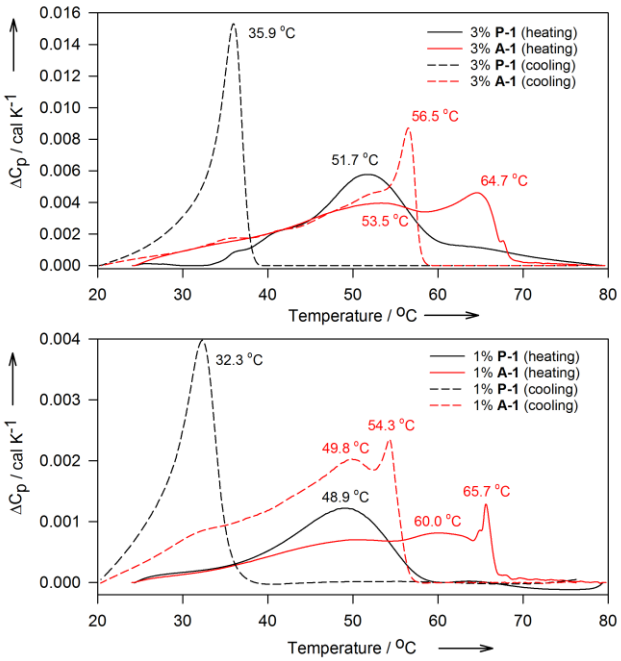

Figure 4. DSC heating (1.0 °C/min) and cooling curves (1.0 °C/min) of (top) 3% toluene gels and (bottom) 1% toluene gels of **P-1** and **A-1** polymers.

Table 3. Enthalpy (ΔH_m) and entropy changes (ΔS_m) of melting of toluene gels of **P-1** and **A-1** polymers.[a]

	ΔH_m (Jg^{-1})	ΔS_m ($Jg^{-1}K^{-1}$)
P-1 (3% in toluene)	25.8	79.6×10^{-3}
A-1 (3% in toluene)	31.4	96.7×10^{-3}
P-1 (1% in toluene)	15.2	47.8×10^{-3}
A-1 (1% in toluene)	18.2	56.1×10^{-3}

[a] Gels were aged at 20 °C for 15 minutes prior to measurements. The integration region was taken from 20 to 80 °C, which encapsulated all the various phase transitions.

The respective enthalpy changes (ΔH_m) and entropy changes (ΔS_m) of the gel melting process were tabulated (Table 3). It was found that melting of the **A-1** gel, which macroscopically behaved as a better organogelator, was more endothermic than that of the **P-1** gel at the same concentration, *i.e.* self-assembly of **A-1** led to a thermodynamically more stable gel aggregates than that of **P-1**. In addition to having a larger ΔH_m, the melting of the **A-1** gel also exhibited a larger ΔS_m value, suggesting that packing of the **A-1** gel was more order than that of the **P-1** gel.

Both the ΔH_m and ΔS_m values of 1.0% gels of polymers were smaller than those obtained at 3.0%, as opposed to the assumption of constant melting enthalpy change predicted by the Eldridge and Ferry's equation,[19] but this could be qualitatively accounted for by a zipper model proposed by Nishinari.[20] This zipper model correlated ΔH_m with a number of parameters including binding energy, number of binding sites, density and rotational freedom of zippers which were taken as rigid rods in crystalline junction zones. Based on statistical mechanics, the observed concentration effect on ΔH_m is closely related to the zipper density. Hence, the reduction of ΔH_m could be attributed to higher chain mobility and fewer crystalline junction zones at a lower gelator concentration.

4. Powder small angle X-ray diffraction analysis (SAXRD). The two polymers were subjected to SAXRD analysis in order to reveal their packing arrangement of the crystallization zone at the molecular level. The SAXRD pattern of a 3% **P-1** xerogel in *para*-xylene showed two peaks at 2θ = 4.2° and 19.2° (Table 4 and SI section 8, Figure S9). The prominent peak at 4.2° was originated from a spacing of 21.0 Å, which was slightly shorter than twice the span of the 5-butylundecyl side chain (~2 × 13 Å). The other peak at 19.2° was much broader, and corresponded to a *d*-spacing of 4.6 Å, which fell into the range of inter-atomic distance of π−π stacking. This result supported the presence of the more crystalline interdigitation of the branched hydrophobic side chains, in addition to the slightly amorphous packing of the backbone aromatic moieties. For **A-1**, whilst the inter-distance of π−π stacking was indistinguishable from that of **P-1**, the crystalline hydrophobic spacing was found to be shorter (18.8 Å) The tighter molecular packing of **A-1** could then account for its higher ΔS_m value obtained in the DSC experiment.

Table 4. SAXRD Data of xerogels prepared from **P-1** and **A-1**.

	First peak		Second peak	
	2θ (°)	*d*-spacing (Å)	2θ (°)	*d*-spacing (Å)
P-1	4.21	21.0	19.23	4.61
A-1	4.70	18.8	19.24	4.61

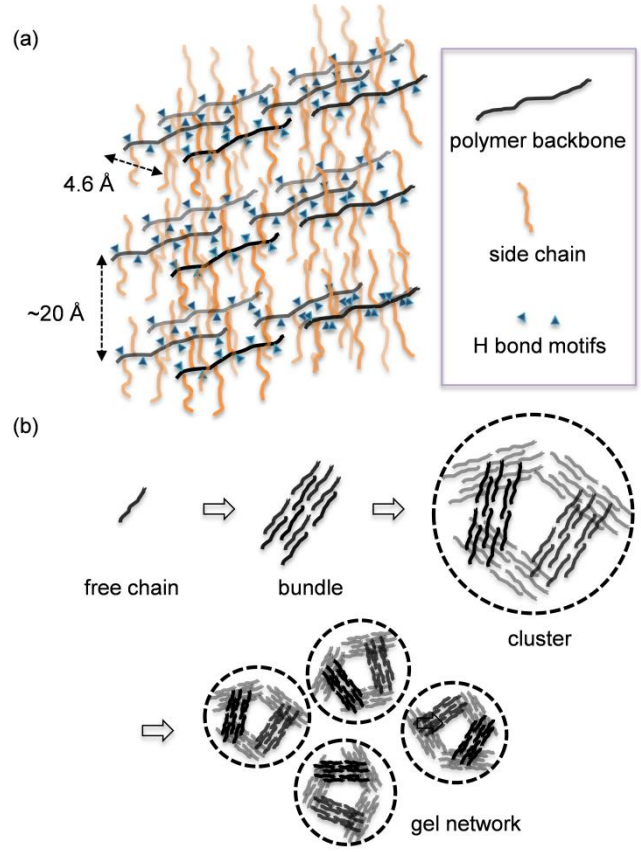

Figure 5. (a) Purposed model of the crystallization zone of the polymer gels of **A-1** and **P-1** and (b) Schematic diagram (side chains are not drawn) showing the formations of gel network via cluster aggregation, cluster formation via bundle association and formation of bundles via polymer chain aggregation (aromatic solvent molecules are omitted for clarity).

5. Gel packing model. On the basis of the above results, a packing model of the polymer gels is proposed (Figure 5). First, the backbone of the polyamides is stiffened due to repulsions among the bulky hydrocarbon side chains, and thus the bottlebrush-shaped macromolecule exists in an extended worm-like conformation. The polymer chains then aggregate through strong H-bonding and π−π stacking interactions along the backbone to produce bundles with an inter-chain spacing of approximately 4.6 Å. Interdigitation of the hydrophobic side chains of the woven fibrillar layers then gives rise to a higher-order layered micro-crystalline cluster in which the inter-layer distance takes the value of approximately 20 Å. The aromatic solvent molecules are entrapped within the matrix via π−π stacking interaction with the aromatic moieties of the polymer and/or with other solvent molecules. These crystalline clusters of different sizes then loosely linked together to form the gel network. Melting of the crystalline zone will then lead to a discontinuous enthalpy change and appears as a sharp transition, while the enthalpy required for cluster-cluster movement is small and heterogeneous, giving rise to rather broad peaks in the DSC profile.

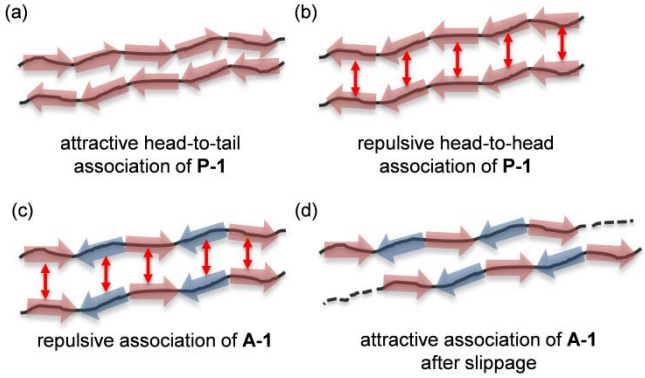

Figure 6. Differential self-association modes of **P-1** and **A-1** polymers.

The differential gelation properties observed for **P-1** and **A-1** must be due to a difference of their macromolecular geometry and/or electronic environment, which led to the formation of clusters of different packing order and stability. However, there is little difference of the spacing between the R^1 and R^2 polymer side chains in **P-1** and **A-1**, and therefore the geometry factor should be less influential. On the other hand, the dipole alignment effect should not be ignored due to its directional and multiplicative nature. Adhered to our original objective, the local dipole-dipole interaction instead of the macro-dipole interaction, will be used to rationalize the observed behavior. There are two possible packing modes for **P-1**, namely, the energetically more favorable head-to-tail (Figure 6a) and the less favorable head-to-head (Figure 6b) associations. However, in a kinetically arrested gel system, there is little chance for one of the chains in the head-to-head mode to tumble over in order to attain the more stable head-to-tail association. Hence, gels prepared from **P-1** should possess both head-to-tail and head-to-head packings. The unfavorable head-to-head arrangement would prevent close interaction between the polymer chains, and was consistent with its less-compact packing nature as shown by the SAXRD data and its smaller enthalpy of melting (ΔH_m) value from DSC data. On the other hand, there is only one association mode for **A-1**. When the initial contact was unfavorable due to dipole-dipole repulsion (Figure 6c), one of the **A-1** polymer chains can slither over the distance of one unit of dipole separation to reach the more stable packing (Figure 6d). The polymer chain does not need to tumble the whole molecule over to attain an enthalpically more favorable association. This rationale was also consistent with the finding that the entropy of melting (ΔS_m) of toluene gel of **A-1** is larger than that of **P-1**, since **P-1** can pack either in head-to-tail or head-to-head fashion, and is therefore less order or entropically higher as compared to **A-1** gel, as the latter could pack in a uniformly head-to-tail fashion. However, it should be emphasized here that the packing outcomes were mainly due to the kinetic entrapment of large polymer molecules in the gel state, and that the same conclusions may not be valid for low molecular weight gel systems, in which the molecular mobility is much higher.

6. Scanning electron microscopy (SEM). Xerogels of the polymers were prepared and subjected to SEM examinations in order to reveal the morphology of their microstructures. All xerogels appeared as clusters of random fibrillar layers throughout the entire structures (see SI section 9, Figure S10). Scrutiny of their SEM images unraveled that **A-1** tended to have a few fibrous structures whereas **P-1** possessed slightly denser morphology.

7. Rheological studies. To further understand the macromolecular motion in the gel state, classical bulk and micro-rheology (diffusion wave spectroscopy) were carried out. The former offers insights on the macroscopic gel mechanical properties at 10−100 microns that are typically the scales of cluster-cluster sliding, while the latter examines the microscopic flow and creeps down to hundredth to several microns, which is within the domain of bundle-bundle interactions.

7A. Bulky rheology. For both 1.0% and 3.0% toluene gels of the two polyamides, the storage modulus (G') values are about 5−10 times of the corresponding loss modulus (G") at the same concentration, manifesting their solid-like behavior (Table 5 and SI section 10, Figure S11). The obtained G'/G" ratios were consistent with the claim by Almdal, who suggested that a gel should possess a G' value greater than the corresponding G" value at least by one order of magnitude.[21] As expected, gels possessed a higher modulus at a higher concentration, as explained by the increase in density of the non-covalent crosslinks. It was also found that the storage modulus of gels of **A-1** was higher than that of **P-1** at the same concentration. Structural strength of the noncovalent network could be also estimated by the flow point at which the structure was irreversibly deformed and the gel started to flow (*i.e.* the crossing over point of curve G' to curve G"). Indeed, gels of **A-1** could sustain three- to six-fold more stress than that of **P-1** at the same concentration.

Table 5. Rheological data of of **P-1** and **A-1** polymer gels in toluene.[a]

	LVE[b]		Flow point[c]
	G' (Pa)	G" (Pa)	Stress (Pa)
P-1 (3%)	946	152	23.2
A-1 (3%)	4339	728	77.5
P-1 (1%)	194	35	6.3
A-1 (1%)	1833	268	42.0

[a] Measurements were done at 25 °C. [b] LVE = linear viscoelastic region, G' and G" were taken as the average over the LVE region. [c] Flow points were determined by the cross-over point of G' and G" curves.

7B. Diffusion wave spectroscopy (DWS). Dimethylsilyl-coated silica microspheres of 1.5 μm in diameter were chosen and imbedded in the toluene gels in the study. The dimethylsilyl groups served to circumvent the interference of H-bonding interaction between the amide moieties on the polymer and the hydroxyl groups on the silica. The size of the microspheres was comparable to the mesh size of the gel network as observed by SEM such that the measured results reflected the change of the gel network structure at the micron scale, which was equivalent to the dimension of the bundle structure inside a large cluster. As the density of the silica particle was about twice as that of toluene, the non-sticky microspheres tended to sediment in pure toluene. However, in the presence of the polymer gelator, the silica particles were able to disperse homogeneously to form a turbid suspension due to the gel network structure.

Preliminary results carried out on 3% gel samples found that the silica beads were too rigidly bound even at the high temperature region (70 °C). Hence only 1.0% partial gel samples of the polymers were subjected to detailed DWS analysis. The mean square displacement (MSD) *vs* lag time plots at various temperatures were shown (Figure 7). First, both **P-1** and **A-1** did not show significant change of MSD even at lag time of 10 s at 25 °C. Secondly, the increment in MSD intensified as the temperature increased, indicating that the transient constraints (H-bonding, π−π stacking and hydrophobic interactions) surrounding the microspheres were loosened at higher temperature, which correlated to bundle-bundle crosslink dissociation. Thirdly, at 25 °C, the MSD value (10^{-8} μm^2) of the **A-1** gel was 10 times smaller than that (10^{-7} μm^2) of the **P-1** gel, while at higher temperature (55 °C), rather surprisingly, a reversal of this trend was observed. However, it was also noted that as the temperature increased, the gel network collapsed and the silica particles began to precipitate. Hence DWS data obtained at higher temperature and long lag time may subject to a higher degree of uncertainty.

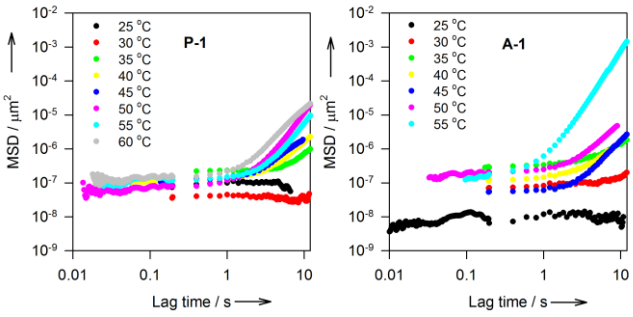

Figure 7. MSD values as a function of lag time in (a) 1.0% toluene partial gel of **P-1** and (b) 1.0% toluene gel of **A-1**.

The MSD data could also be transformed to oscillatory rheograms by the generalized Stokes-Einstein equation. The transition from stagnant behavior at short lag time to diffusive behavior at long lag time resembled the frequency crossovers in the terminal flow region, where the liquid character prevailed over solid character as the frequency decreased (see SI section 11, Figure S12). The crossover frequency marked the characteristic relaxation time of a network, and could be inferred to the rate of dissociation of the transient crosslinks. In general, the crossover frequency increased with temperature as the

crosslinks were loosened by thermal agitation. The corresponding relaxation times were then fitted into the Eyring equation with good correlation coefficients (r^2 = 0.85−0.93). The obtained activation enthalpy ($\Delta H^{\ddagger}$) and entropy ($\Delta S^{\ddagger}$) reflected the kinetics of the bundle-bundle breaking down process (Table 6 and SI section 11, Figure S13). The activation enthalpy ($\Delta H^{\ddagger}$) of the breaking down of the transient crosslinking of **P-1** (2.8 Jg^{-1}) was found to be lower than that of **A-1** (4.6 Jg^{-1}), whereas the activation entropy ($\Delta S^{\ddagger}$) for **P-1** and **A-1** was −5.1 and −0.87 $mJK^{-1}g^{-1}$, respectively. The negative values of $\Delta S^{\ddagger}$ implied that the transition states had higher packing order than the ground states, which can be rationalized by the fact that the prepared gels were in a kinetically-trapped, less order state during preparation by ambient temperature cooling. As a result, the various dipole-dipole and H-bonding interactions were not geometrically optimized and hence the ground states were structurally less ordered. The fact that **P-1** possessed a significantly larger drop in activation entropy (*i.e.* $\Delta S^{\ddagger}$ is more negative) towards dissociation indicated its gel packing was much less order than that of **A-1**, a fact that was already confirmed by SAXRD and gel strength measurements described earlier. It should be noted that phase transitions probed by the DWS method are different from those by DSC measurement. The latter determines the total enthalpy and entropy of all phase transition processes, while the former focuses only on the corresponding processes originated from bundle-bundle interaction.

Table 6. Activation enthalpy ($\Delta H^{\ddagger}$) and entropy ($\Delta S^{\ddagger}$) of intra-cluster crosslink dissociation of 1% **P-1** and **A-1** polymer partial gels in toluene.[a]

	$\Delta H^{\ddagger}$ (Jg^{-1}) [b]	$\Delta S^{\ddagger}$ ($mJK^{-1}g^{-1}$) [b]
P-1	2.80 ± 0.57	−5.10 ± 1.56
A-1	4.60 ± 0.72	−0.87 ± 0.18

[a] Only the data obtained from 25−60 °C (before tracer particles completely sank) were fitted into Eyring equation. Error terms were calculated at one standard error. [b] Quantities relative to per gram of polyamide.

The lower $\Delta H^{\ddagger}$ value of **P-1** towards inter-bundle sliding could be again rationalized by the dipolar model proposed earlier (Figure 8). Upon application of shear force, the chains were disengaged and eventually manifested a liquid flow. If the **P-1** chains are aligned in the less stable head-to-head fashion, chain sliding is enthalpically favorable due to the already repulsive interaction between the chains (not shown in Figure 8). If the chains are aligned in a head-to-tail fashion, the **P-1** chain only needed to slither one dipole unit to attain the next stable configuration (Figure 8a), whereas for **A-1** chains, there existed strong dipolar repulsion in the course of sliding over one dipole unit, and a stable state could only be attained when the chain slipped over two dipole units (Figure 8b). As a result, crosslink dissociation was enthalpically disfavored for **A-1**.

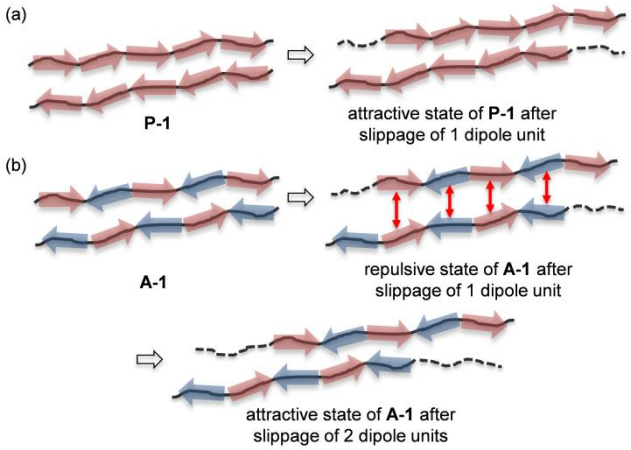

Figure 8. Proposed model of dissociation and association of transient bundle-bundle interaction in (a) **P-1** and (b) **A-1** polymers.

Self-Sorting of P-1 and A-1 polymers

Formation of mixed gel systems has already been reported for small molecules,[22] polymers and biopolymers.[23] The problem is complicated by whether the individual component is a gelator on its own or not. Various models had been proposed to predict the property of the resulting mixed gel systems. These include the non-self-association,[24] single-self and cross-association,[25] and double-self and cross-association models.[26] One key question of such mixed gel systems is whether the components are fully miscible with each other or self-sort which results in phase separation. Generally, the greater the structural difference between the two molecular species, the higher the tendency of the mixed system to exhibit self-sorting. This is because greater structural difference will normally lead to a higher chance of having immiscible functionalities in the two components. While self-sorting is a commonplace in small molecules, it is less prevalent in synthetic macromolecules. Notable examples are narcissistic self-sortings of norbornene copolymers,[27] of bisurea-based bolaamphiphilic polymers[28] and of bisurea-based thermoplastic elastomers.[29] On the other hand, example of social self-sorting has also been reported in the case of bisurea-based thermoplastic elastomers.[30] We earlier disclosed that oligo(triazole-amide)s of significantly different number of H-bond units did exhibit self-sorting in a 1:1 mixed gel system.[7] In the case of the **P-1** and **A-1** polymers reported here, we are therefore interested to know whether a mere difference in the monomer dipole alignment can promote self-sorting in their mixed gel systems.

Preliminary examination of the DSC heating curve of the 1:1 mixed gel did not give any conclusive evidence due to multiple phase transitions that were very close to each other. However, self-sorting was highlighted by the cooling curve (Figure 9). Two distinct peaks of similar size and shape were observed. If the mixture was homogeneous, one average broad transition peak would have been expected. As it turned out, the transition maxima of the mixed gel were shifted towards lower temperature in comparison to their respective pure gels, suggesting that the

inter-molecular and inter-cluster interactions were slightly disrupted. The efficacy of self-sorting could be reflected by the magnitude of enthalpy and entropy changes of gelation (Table 7). As can be seen, the magnitude of the enthalpy of gelation from the 1:1 mixture gel (-17.7 Jg^{-1}) was higher than that of the average of pure **P-1** and **A-1** (-22.5 Jg^{-1}). Hence the mixing process resulted in a positive rise of enthalpy (4.7 Jg^{-1}). Incidentally, the mixing process also gave a positive rise in entropy (14.5×10^{-3} $Jg^{-1}K^{-1}$). At 25 °C, the rise of the Gibbs free energy of mixing can be calculated as +0.48 Jg^{-1}, indicating the mixing was an unspontaneous process (additional experimental results of the self-sorting property can be found in SI, section 7.III).

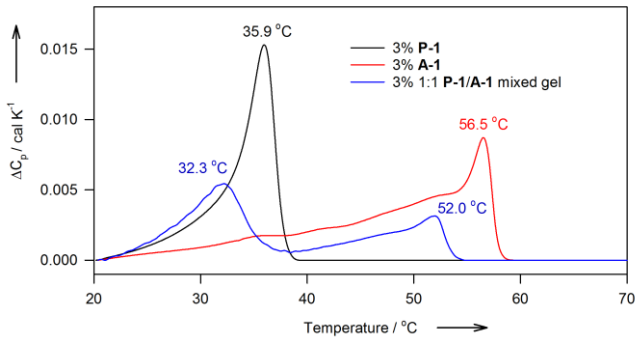

Figure 9. DSC exotherms of 1:1 mixed gel of **P-1** and **A-1** (blue), superimposed with that of pure gels of **P-1** (black) and **A-1** (red) at 3.0% concentration.

Table 7. Enthalpy and entropy changes of gelation of 3% toluene gel of **P-1**, **A-1** and their 1:1 mixture.[a]

	ΔH_g (Jg^{-1})	ΔS_g ($Jg^{-1}K^{-1}$)
P-1 (3% in toluene)	−20.1	-65.6×10^{-3}
A-1 (3% in toluene)	−24.8	-77.7×10^{-3}
1:1 mixed gel of **P-1** and **A-1** (3% in toluene)	−17.7	-57.2×10^{-3}
Average value of pure **P-1** and **A-1** (3% in toluene)	−22.5	-71.7×10^{-3}

[a] Gels were annealed at 80 °C for 15 minutes prior to measurements. The integration region was taken from 20−80 °C.

The origin of the unfavorable mixing of the two polymers can be rationalized by the unfavorable dipole-dipole interaction due to hetero-association, leading to reduced inter-chains and inter-clusters association (Figure 10). The repulsion was arisen from mismatches of dipole motifs when the parallel and antiparallel strands are closed to each other, and it also served as an impetus to drive self-sorting. Sliding of the polymer strands cannot eliminate such unfavorable interactions.

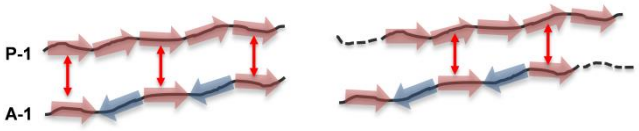

Figure 10. (left) Unfavorable dipole-dipole interactions between **P-1** and **A-1** polymers. (right) Such unfavorable interactions still persist even after chain slippage.

Conclusions

Two isomeric polyamides **P-1** and **A-1**, with the backone-dipoles aligned in parallel and antiparallel fashion, respectively, were successfully prepared and characterized. The two polymers were found to form strong physical gels with a wide variety of aromatic solvents. Despite their close structural similarity, T_m, DSC and bulky rheology measurements all revealed that the gels obtained from **A-1** were consistently stronger than those from **P-1**. Based on FT-IR and SAXRD experiments, gelation was due to H-bonding, π−π stacking interactions and hydrophobic side chain interdigitation. DSC study also revealed that the polymer gels so prepared by ambient temperature cooling were in a kinetically trapped state. Gelation involved first the association of individual polymer chains to produce bundles which subsequently formed crystalline clusters of different sizes. These clusters then further aggregated in an amorphous manner to produce the bulk gel network. DWS study found that the activation enthalpy of the intra-cluster melting process of **A-1** was higher than that of **P-1**. Incidentally, the two polymers were also found to exhibit self-sorting in a 1:1 mixed gel system. The differential gelation properties and the self-sorting phenomenon could be readily rationalized by local dipole-dipole interactions that were originated from the parallel or antiparallel alignment of the backbone dipoles. As it appears, there is no need to invoke the macro-dipole model in order to explain the observed differential properties. Admittedly this may be a simplified model, but it serves the purpose to rationalize the property of a polymer system which is less complicated than that of a protein system. In the protein case, additional dipolar influences from the polar side chains and polar water molecules cannot be simply ignored. The results reported here indicating that local dipole-dipole interaction is a critical factor that can strongly affect the self-association and supramolecular properties of polymers. Furthermore, a subtly small change in the polymer structure, such as reversing the direction of the dipole alignment, can lead to highly efficient molecular self-sorting in polymer gels.

Experimental Section

Details of the polymer syntheses, compound characterizations and gelation property studies are given in the electronic supplementary information (SI).

Acknowledgements

We thank the Research Grants Council (RGC Ref No 400712) for the financial support, Ms Yan-Lam Lau for synthesizing some of the intermediates, and Profs. To Ngai and Zhaoyan Sun for their helpful discussion.

Keywords: supramolecular chemistry • polyamide • physical gel • self-sorting • dipole-dipole interaction

[1] a) J. D. Sipe, A. S. Cohen, *J. Struct. Biol.* **2000**, *130*, 88–98; b) J.-C. Rochert, P. T. Jr. Lansbury, T. Peter, *Curr. Opin. Struct. Biol.* **2000**, *10*, 60–68; c) F. Chiti, C. M. Dobson, *Ann. Rev. Biochem.* **2006**, *75*, 333–366.

[2] D. Wang, Y. Yuan, Y. Mardiyati, C. Bubeck, K. Koynov, *Macromolecules* **2013**, *46*, 6217−6224; b) Y. Yao, H. Dong, W. Hu, *Polym. Chem.* **2013**, *4*, 5197−5205.

[3] G. Tillet, B. Boutevin, B. Ameduri, *Prog. Polym. Sci.* **2011**, *36*, 191–217.

[4] For reviews and monographs on thermoreversible gelation of polymers and biopolymers, see: a) J. Spěváček, B. Schneider, *Adv. Colloid Interface Sci.* **1987**, *27*, 81–150; b) J.-M. Guenet, *Thermoreversible Gelation of Polymers and Biopolymers*, Academic Press, London, **1992**; c) M. Suzuki, K. Hanabusa, *Chem. Soc. Rev.* **2010**, *39*, 455–463; d) A. Noro, M. Hayashi, Y. Matsushita, *Soft Matter* **2012**, *8*, 6416–6429.

[5] For reviews and monographs on low molecular weight gels, see: a) P. Terech, R. G. Weiss, *Chem. Rev.* **1997**, *97*, 3133–3160; b) N. M. Sangeetha, U. Maitra, *Chem. Soc. Rev.* **2005**, *34*, 821–836; c) R. G. Weiss, P. Terech, Eds. *Molecular Gels. Materials with Self-Assembled Fibrillar Networks*, Springer, Dordrecht, The Netherlands, **2005**; d) M. George, R. G. Weiss, *Acc. Chem. Res.* **2006**, *39*, 489–497; e) P. Dastidar, *Chem. Soc. Rev*. **2008**, *37*, 2699–2715.

[6] H.-F. Chow, T.-K. Chui, Q. Qi, *Synlett* **2014**, *25*, 2246–2255.

[7] J. Zhang, H.-F. Chow, M.-C. Chan, G. K.-W. Chow, D. Kuck, *Chem. Eur. J.* **2013**, *19*, 15019–15025.

[8] S.-L. Yim, H.-F. Chow, M.-C. Chan, C.-M. Che, K.-H. Low, *Chem. Eur. J.* **2013**, *19*, 2478–2486.

[9] K.-N. Lau, H.-F. Chow, M.-C. Chan, K.-W. Wong, *Angew. Chem.* **2008**, *120*, 7018–7022; *Angew. Chem. Int. Ed.* **2008**, *47*, 6912–6916.

[10] H.-F. Chow, K.-N. Lau, M.-C. Chan, *Chem. Eur. J.* **2011**, *17*, 8395–8403.

[11] R. P. Sheridan, R. M. Levy, F. R. Salemme, *Proc. Natl. Acad. Sci. USA* **1982**, *79*, 4545–4549.

[12] W. G. J. Hol, P. T. van Duijnen, H. J. C. Berendsen, *Nature* **1978**, *273*, 443–446.

[13] E. G. Baker, G. J. Bartlett, M. P. Crump, R. B. Sessions, N. Linden, C. F. J. Faul, D. N. Woolfson, *Nat. Chem. Biol.* **2015**, *11*, 221–228.

[14] S. S. Sheiko, B. S. Sumerlin, K. Matyjaszewski *Prog. Polym. Sci.* **2008**, *33*, 759–785.

[15] Polymer chains containing only $v_{\parallel}$ dipoles are called type-A chains; while those containing solely $v_{\perp}$ dipoles are called type–B chains. The dipolar effects of type-A and type-B chains on their properties had been reported, see a) W. H. Stockmayer *Pure. Appl. Chem.* **1967**, *15*, 539–554; b) K. Adachi, T. Kotaka, *Prog. Polym. Sci.* **1993**, *18*. 585–662.

[16] a) T. Sakai, J.-i. Horinaka, T. Takigawa, *Polym. J.* **2015**, *47*, 244–248; b) A. H. Clark, S. B. Ross-Murphy, *Adv. Polym. Sci.* **1987**, *83*, 57–192.

[17] F. M. Menger, K. L. Caran, *J. Am. Chem. Soc.* **2000**, *122*, 11679–11691.

[18] a) P. J. Flory, *Faraday Discuss. Chem. Soc.* **1974**, *57*, 7–18; b) K. te Nijenhuis, *Adv. Polym. Sci.* **1997**, *130*, 1–235.

[19] J. E. Eldridge, J. D. Ferry, *J. Phys. Chem.* **1954**, *58*, 992–995.

[20] K. Nishinari, S. Koide, P. A. Williams, G. O. Phillips, *J. Phys. France* **1990**, *51*, 1759–1768.

[21] K. Almdal, J. Dyre, S. Hvidt, O. Kramer, *Polym. Gels Netw.* **1993**, *1*, 5–17.

[22] L. E. Buerkle, S. J. Rowan, *Chem. Soc. Rev.* **2012**, *41*, 6089–6102.

[23] *Biopolymer Mixtures*; S. E. Harding, S. E. Hill, J. R. Mitchell, Eds.; Nottingham University Press, Nottingham, England, **1995**.

[24] C.-F. Mao, J.-C. Chen, *J. Appl. Polym. Sci.* **2006**, *99*, 2771–2781.

[25] C.-F. Mao, *J. Polym. Sci. Polym. Phys.* **2008**, *46*, 80–91.

[26] Y. Park, B. Veytsman, M. Coleman, P. Painter, *Macromolecules* **2005**, *38*, 3703–3707.

[27] a) C. Burd, M. Weck *Macromolecules* **2005**, *38*, 7225–7230; b) C. R. South, C. Burd, M. Weck, *Acc. Chem. Res.* **2007**, *40*, 63–74.

[28] A. Pal, S. Karthikeyan, R. P. Sijbesma *J. Am. Chem. Soc.* **2010**, *132*, 7842–7843.

[29] N. E. Botterhuis, S. Karthikeyan, A. J. H. Spiering, R. P. Sijbesma *Macromolecules* **2010**, *43*¸ 745–751.

[30] E. Wisse, L. E. Govaert, H. E. H. Meijer, E. W. Meijer *Macromolecules* **2006**, *39*, 7425–7432.

10.1002/chem.201605819

WILEY-VCH

Entry for the Table of Contents (Please choose one layout)

Layout 1:

FULL PAPER

Text for Table of Contents

((Insert TOC Graphic here: max. width: 5.5 cm; max. height: 5.0 cm))

*Author(s), Corresponding Author(s)**

Page No. – Page No.

Title

Layout 2:

FULL PAPER

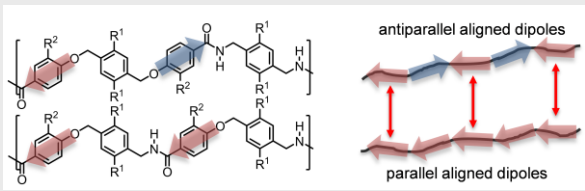

Two isomeric polyamides, one with the backbone dipoles aligned in antiparallel and the other in parallel fashion, were found to show differential organogelation properties. They also exhibited self-sorting in their 1:1 mixed toluene gel. These observations can be rationalized by the different local dipole-dipole interactions manifested in the pure gel and the mixed gel systems.

Chui-Fan Leung,[a] and Hak-Fun Chow[a]*

Page No. – Page No.

Differential Gelation and Self-Sorting Properties of Two Isomeric Polyamides Due to the Parallel *vs* Anti-Parallel Alignment of Backbone Dipoles